# Phase diagram of the random field Ising model on the Bethe lattice

Thomas Nowotny, Heiko Patzlaff, and Ulrich Behn
*Institut für Theoretische Physik, Universität Leipzig, P. O. Box 920, 04109 Leipzig, Germany*
(Received 6 June 2001; revised manuscript received 13 September 2001; published 19 December 2001)

The phase diagram of the random field Ising model on the Bethe lattice with a symmetric dichotomous random field is closely investigated with respect to the transition between the ferromagnetic and paramagnetic regimes. Refining arguments of Bleher, Ruiz, and Zagrebnov [J. Stat. Phys. **93**, 33 (1998)], an exact upper bound for the existence of a unique paramagnetic phase is found, which considerably improves the earlier results. Several numerical estimates of transition lines between a ferromagnetic and a paramagnetic regime are presented. The results obtained do not coincide with the lower bound for the onset of ferromagnetism proposed by Bruinsma [Phys. Rev. B **30**, 289 (1984)]. If Bruinsma's estimate proves correct, this would hint at a region of coexistence of stable ferromagnetic phases and a stable paramagnetic phase.

DOI: 10.1103/PhysRevE.65.016127 PACS number(s): 05.50.+q, 05.45.Df, 75.10.Nr, 05.70.Fh

## I. INTRODUCTION

The random field Ising model (RFIM) has been studied extensively in theory [1] as well as in experiment [2]. The one-dimensional model [5–16] can be reformulated as a random iterated function system (RIFS) for an effective field [5,7–9]. The reformulation leads to an iteration of first order whereas standard transfer matrix methods lead to iterated function systems of second order. This considerable simplification allows deep insights into the effects of quenched random fields on local thermodynamic quantities.

Being one dimensional, the Ising chain has no phase transitions for finite temperature though. The RFIM on the Bethe lattice, to the contrary, exhibits for not too high temperature at least a phase transition from ferromagnetic behavior for small random fields to paramagnetic behavior for large fields [3,4,17]. The phase diagram is probably much richer [18]. For $T=0$ hysteresis effects have been found and investigated in detail [21].

The Bethe lattice (Cayley tree) is uniquely characterized by the two properties that it is an infinite simple graph with constant vertex degree and that it contains no loops. It is of order or degree $k$ if the vertex degree is $k+1$. The Bethe lattice of degree $k=1$ is the one-dimensional lattice and the Bethe lattice of degree $k=2$ the well known binary tree. Because the Bethe lattice contains no loops, the RFIM on the Bethe lattice can be reformulated to a (generalized) RIFS [3,4,19] for the effective field, as in the one-dimensional model [7,9]. Therefore, the same powerful techniques as in the one-dimensional case can be applied to gain insight into the mechanisms driving the phase transition. Nevertheless the exact transition line in the $(T,h)$ parameter plane is still not known. Recently, exact lower bounds for the existence of a stable ferromagnetic phase as well as exact upper bounds for the existence of a stable paramagnetic phase were proved [3]. We present an improved upper bound for the existence of a stable paramagnetic phase based on this approach. These bounds are still far from the region where the transition is expected though. Therefore, we also develop several criteria to detect the phase transition line numerically. It turns out that the results obtained, while being consistent with each other, disagree significantly with an early result by Bruinsma [4], who calculated a lower bound for the onset of ferromagnetic behavior. As Bruinsma's argument rests on the differentiability of the density of the invariant measure of the RIFS, which was proved only for small $h$ and near $T_c$, there are two possible interpretations. Either Bruinsma's bound is not true outside the proven region of validity and the transition from ferromagnetic to paramagnetic behavior takes place at the smaller random field values found in our numerical results, or there is a region of coexistence of stable ferromagnetic phases with a stable paramagnetic phase, implying a phase transition of first order in this region.

The paper is organized as follows. After introducing the model and our notation in Sec. II we present the improved exact upper bounds for the onset of paramagnetism in Sec. III. In Sec. IV we give three criteria to estimate the transition line between the ferromagnetic and paramagnetic regimes. The expectation value of the local magnetization is calculated directly and we extract an estimate for the region of a stable ferromagnetic phase. We then study the average contractivity of the RIFS of the effective field. This leads to an estimate for the appearance of a stable paramagnetic phase for increasing random field strength $h$. The third criterion is the independence of the effective field from boundary conditions. It also provides an estimate for the stability region of the paramagnetic phase. The implications of our results in comparison to Bruinsma's approach are discussed in detail in the concluding Sec. V.

## II. MODEL

The formulation of the RFIM on a Bethe lattice requires some notation for the underlying lattice. By $V$ we denote the set of vertices of the Bethe lattice and $d(y,z)$ is the natural metric on the lattice given by the length of the unique path connecting $y$ and $z$. Furthermore, $V_R := \{y \in V : d(y,y_0) \leq R\}$ denotes the ball of radius $R$ around some arbitrarily chosen central vertex $y_0$ and $\partial V_R := \{y \in V : d(y,y_0) = R\}$ its boundary, the sphere of radius $R$. In the following it will be useful to decompose $V$ into two subtrees $V^+$ and $V^-$ with roots $y_0$ and $z_0$ in the way illustrated in Fig. 1.

Introducing the notation $\mathcal{S}(y) := \{z \in \partial V_{R+1} : d(y,z) = 1\}$

 

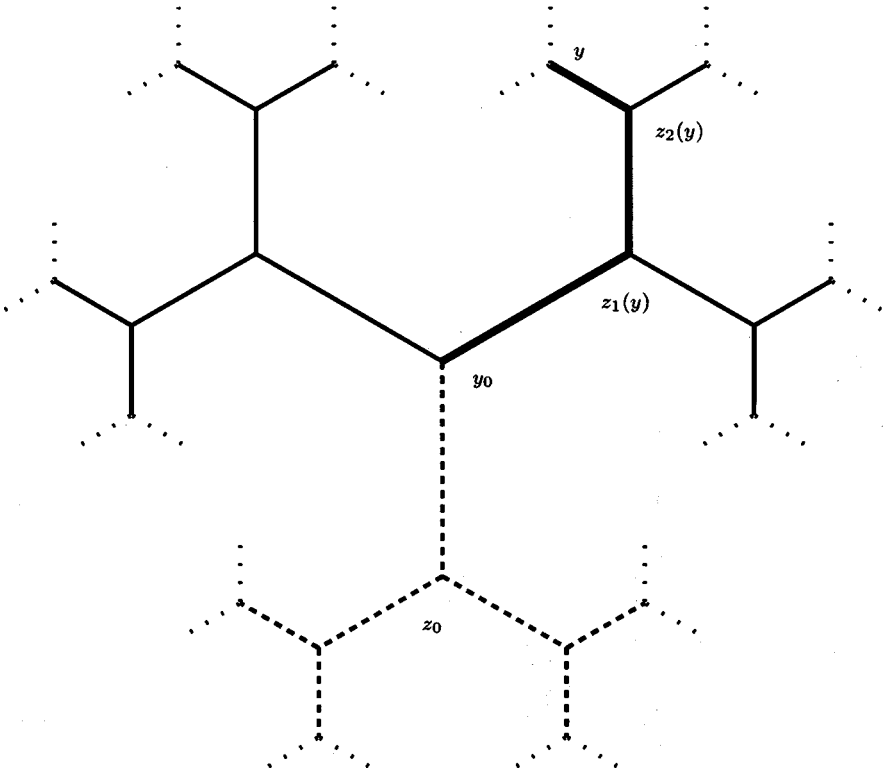


FIG. 1. Bethe lattice of degree $k=2$. The solid lines mark the part of the lattice denoted by $V^+$ and the dashed lines the part denoted by $V^-$. The roots of the two subtrees are denoted by $y_0$ and $z_0$, respectively. The thick line shows the unique path from a vertex $y \in \partial V_3$ at the boundary to the central vertex $y_0$ to illustrate the labeling along the path used in Sec. III.

for the successors of $y \in \partial V_R$, the Hamiltonian of the RFIM on the Bethe lattice reads

$$H_R(\{s_y\}_{y \in V_R}) = -\sum_{\substack{y \in V_{R-1} \\ z \in \mathcal{S}(y)}} J s_y s_z - \sum_{y \in V_{R-1}} h_y s_y - \sum_{y \in \partial V_R} x_y^b s_y, \tag{1}$$

where $s_y$ denotes the classical spin at vertex $y$ taking values $\pm 1$, $J$ is the coupling strength, $h_y$ is the random field at site $y$, and $x_y^b$ is the field at the boundary encoding the chosen boundary conditions. We restrict ourselves to independent, identically distributed, symmetric dichotomous random fields, i.e., $h_y = \pm h$ with probability 1/2. The canonical partition function

$$Z_R := \sum_{\{s_y\}_{y \in V_R}} \exp[-\beta H_R(\{s_y\})], \tag{2}$$

where $\beta = (k_B T)^{-1}$ is the inverse temperature, can be reformulated by a method first introduced by Ruján [7] for the one-dimensional RFIM, resulting in

$$Z_R = \sum_{s_{y_0} = \pm 1} \exp\beta \left\{ [x_{y_0}^{(R)} + A(x_{z_0}^{(R)})] s_{y_0} + \sum_{y \in V_R \setminus \{y_0\}} B(x_y^{(R)}) \right\}, \tag{3}$$

where the effective fields $x_z^{(R)}$ are determined by the generalized RIFS

$$x_y^{(R)} = \sum_{z \in \mathcal{S}(y)} A(x_z^{(R)}) + h_y, \tag{4}$$

with boundary conditions $x_y^{(R)} = x_y^b$ for $y \in \partial V_R$. The functions $A$ and $B$ are given by

$$A(x) = (2\beta)^{-1} \ln[\cosh \beta(x+J)/\cosh \beta(x-J)], \tag{5}$$

$$B(x) = (2\beta)^{-1} \ln[4 \cosh \beta(x+J) \cosh \beta(x-J)]. \tag{6}$$

Note that the upper index $^{(R)}$ of the effective field refers to the radius of the sphere where the boundary conditions are fixed. The partition function in form (3) is a partition function of one spin $s_{y_0}$ in two effective fields $x_{y_0}^{(R)}$ and $A(x_{z_0}^{(R)})$ which are both determined through RIFS (4). The sum in Eq. (4) implies that, although $|A'| < 1$ for nonzero $T$, the RIFS is not necessarily contractive, in contrast to the one-dimensional case. A loss of contractivity indicates a phase transition, as is explained in more detail below.

Since they are functions of the random fields $h_y$, the effective fields are random variables (RVs) on the random field probability space and iteration (4) induces a Frobenius-Perron or Chapman-Kolmogorov equation for their probability measure:

$$\nu_y^{(R)}(X) = \sum_{h_y = \pm h} \frac{1}{2} \left( \prod_{z \in \mathcal{S}(y)}^{*} A_{\#} \nu_z^{(R)} \right)(X - h_y), \tag{7}$$

where $\Pi^*$ denotes the convolution product of measures, $X$ is some measurable set, $X - h_y := \{x - h_y | x \in X\}$, and $A_{\#}$ is the induced mapping of $A$ on measures, i.e., $A_{\#}\mu(X) := \mu(A^{-1}(X))$. The measures of the effective fields at the boundary are fixed by boundary conditions, e.g., as $\nu_y^{(R)} = \delta_{x_y^b}$, the Dirac measure at $x_y^b$. Any other choice of the RVs $x_y^b$ is also possible, though.

It was proved in Ref. [3] that the existence of limiting Gibbs measures with finite restrictions compatible with Eqs. (1) and (2) (cf. Ref. [20]) implies the weak convergence of the RVs $x_y^{(R)}$, i.e., the weak convergence of the measures $\nu_y^{(R)}$ to measures $\nu_y$ in the limit $R\to\infty$. For homogeneous boundary conditions $x_y^b \equiv x^b$ for all $y\in V$, the measures $\nu_y$ are all identical and will be denoted by $\nu$.

Before we can present our results on phase transitions in the RFIM on the Bethe lattice some more properties of RIFS (4) and the function $A$ are necessary. $A(x)$ is a monotonic function in $x$. For a given random field configuration $\{h_y\}_{y\in V_R^+}=\{\sigma_y h\}_{y\in V_R^+}$, $\sigma_y=\pm$, we denote the composite function mapping the effective fields in $\partial V_{R+1}^+$ to the effective field at $y_0$ by $f_{\{\sigma\}_R}$. Here, $\{\sigma\}_R$ is the tree of $k^{R+1}-1$ symbols $\pm$ characterizing the configuration of the random field and $k$ is the degree of the Bethe lattice. These composite functions are monotonic in the sense that if $x_y^b \geqslant x_y'^b$ for all $y\in\partial V_{R+1}^+$ then $f_{\{\sigma\}_R}(\{x_y^b\})\geqslant f_{\{\sigma\}_R}(\{x_y'^b\})$. In the same way they are monotonic with respect to the random field, $f_{\{\sigma\}_R}(\{x_y^b\})\geqslant f_{\{\sigma'\}_R}(\{x_y^b\})$ if $\sigma_y\geqslant\sigma_y'$ for all $y\in V_R^+$. Furthermore, there exists an invariant interval $I=[x_-^*,x_+^*]$ with the property that if $x_y\in I$ for all $y\in\partial V_{R+1}^+$ then also $f_{\{\sigma\}_R}(\{x_y\})\in I$ for any random field configuration $\{\sigma\}_R$. Here, $x_-^*$ and $x_+^*$ are the fixed points of the composite functions for homogeneous $\{-\}$ and homogeneous $\{+\}$ configurations of the random field, respectively. Since $A(x)=-A(-x)$, these fixed points are symmetric, $x_-^*=-x_+^*$.

## III. UPPER BOUNDS FOR THE EXISTENCE OF A UNIQUE PARAMAGNETIC PHASE

In this section we present an exact upper bound for the existence of a unique paramagnetic phase in terms of the random field strength $h$. This bound improves earlier results in Ref. [3].

Throughout this section we will use effective fields $g_y := A(x_y)$ in close analogy to the notation in Ref. [3]. This has some advantages in the calculation, which will become clear below. Iteration (4) for $g_y$ reads

$$g_y^{(R)}=\begin{cases} g_y^b & \text{for } y\in\partial V_R, \\ A\left(\sum_{z\in\mathcal{S}(y)} g_z^{(R)}+h_y\right) & \text{otherwise,}\end{cases} \tag{8}$$

and we denote the composite functions mapping the effective fields $\{g_y\}_{y\in\partial V_{R+1}^+}$ to $g_{y_0}$ by $\tilde{f}_{\{\sigma\}_R}$. They have the same monotonicity properties as the composite functions $f_{\{\sigma\}_R}$.

In order to prove the existence of a unique paramagnetic phase it is sufficient to show that the RVs $g_y$ do not depend on the boundary conditions $\{g_y^b\}$ in the limit $R\to\infty$ for any choice of the boundary conditions. We use the notation $g_y^+$ for the effective field at $y\in V$ for homogeneous boundary conditions $g_y^b\equiv g_+^*$ in the limit $R\to\infty$ and $g_y^-$ for the effective field resulting from the corresponding negative boundary conditions $g_y^b\equiv g_-^*$ where $g_+^*=A(x_+^*)$ and $g_-^*=A(x_-^*)$. For $g_{y_0}^+$ and $g_{y_0}^-$ we use the shorthand notations $g^+$ and $g^-$. Note that the dependence of the effective fields on the random field configurations is suppressed in this notation.

Inspired by the proof for the existence of a unique paramagnetic phase for the RFIM on the Bethe lattice of degree 2 for almost all random field configurations and $2<h<3$ in Ref. [3], we investigate the expectation value

$$\mathbb{E}_{\{\sigma\}}(|g^+-g^-|). \tag{9}$$

The monotonicity of the composite functions $\tilde{f}_{\{\sigma\}_R}$ implies that, if this expectation value is zero for the two extremal boundary conditions chosen above, then it is zero for any two sets of boundary conditions. This then implies that the RV $g_{y_0}$ is independent of the boundary conditions for almost all random field configurations. The goal of this section is therefore to find a criterion for the random field strength $h$ which implies that expectation value (9) is zero. Because of the monotonicity of the composite functions $\tilde{f}_{\{\sigma\}_R}$ we have $g^+\geqslant g^-$ and thus $|g^+-g^-|=g^+-g^-$. Therefore, we consider

$$\begin{aligned}\mathbb{E}_{\{\sigma\}}(g^+-g^-)&=\int d\eta(\{\sigma\})(g^+-g^-)\\ &=\sum_{\{\sigma\}_R}\int_{\{\tilde\sigma\}_R=\{\sigma\}_R} d\eta(\{\tilde\sigma\})[g^+(\{\tilde\sigma\})\\ &\quad -g^-(\{\tilde\sigma\})],\end{aligned} \tag{10}$$

where $\eta$ is the product measure of the probability measures of the random fields $h_y=\sigma_y h$. In the second step the integration was split up into a sum of a finite number of integrals over sets of configurations with fixed symbols $\{\sigma\}_R$ in $V_R$ and arbitrary $\{\tilde\sigma\}\in V\backslash V_R$. Using recursion relation (4) the integrand can be expressed as a function of the effective fields $\{g_y^+\}_{y\in\partial V_R}$ on the boundary of $V_R$:

$$\begin{aligned}g^+(\{\tilde\sigma\})-g^-(\{\tilde\sigma\})&=\tilde{f}_{\{\tilde\sigma\}_{R-1}}(\{g_y^+\}_{y\in\partial V_R})\\ &\quad-\tilde{f}_{\{\tilde\sigma\}_{R-1}}(\{g_y^-\}_{y\in\partial V_R})\\ &=\sum_{y\in\partial V_R}\partial_{g_y}\tilde{f}_{\{\tilde\sigma\}_{R-1}}(\{\delta_z\}_{z\in\partial V_R})\\ &\quad\times(g_y^+-g_y^-).\end{aligned} \tag{11}$$

In the second step the mean value theorem has been used for $\tilde{f}_{\{\tilde\sigma\}_R}$ and $\delta_z\in[g_z^-,g_z^+]$ are appropriately chosen. The partial derivatives in Eq. (11) are bounded from above by $\Pi_{l=0}^{R-1}A'^{(R)}_{z_l(y)_{\max}}$, where $A'^{(R)}_{z_l(y)_{\max}}$ is an upper bound on the maximum of $A'(x)$ for $x\in[g^-_{z_l(y)},g^+_{z_l(y)}]$, the interval of possible values of the effective field at the vertices $z_l(y)$ along the unique path from $y$ to $y_0$ (see Appendix subsection 1 for details). This bound depends only on $\{\tilde\sigma\}_R=\{\sigma\}_R$ and hence is independent of the integration. Thus,

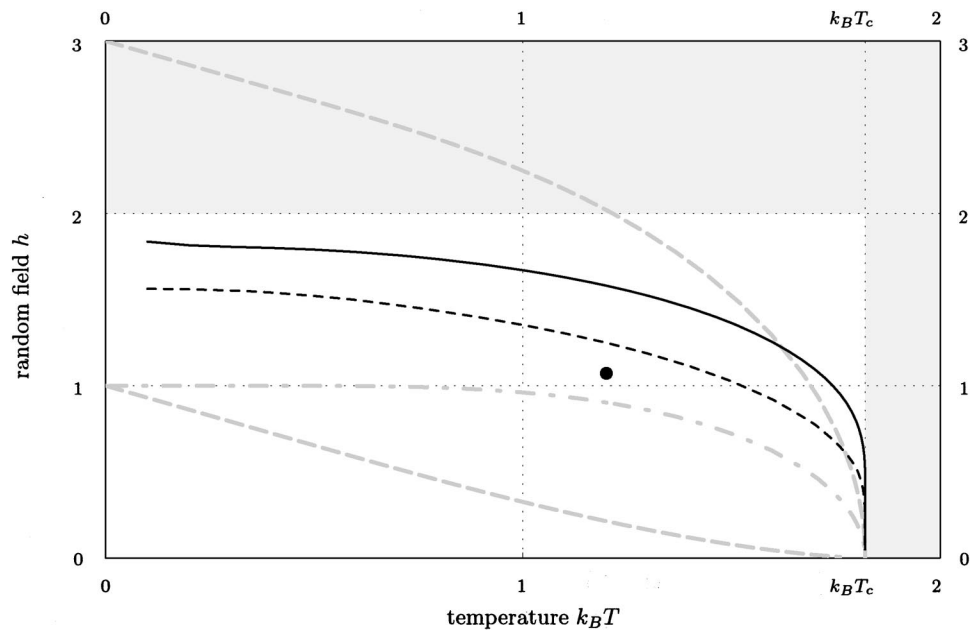


FIG. 2. Exact upper bound for the existence of a stable paramagnetic phase on the Bethe lattice of degree $k=2$ (solid line). The bound was obtained as described in the text with all random field configurations at $R=4$. The dashed line is a similar upper bound obtained by considering a sample of $10^4$ realizations of the random field at $R=11$ using complete sum (13). Close to $T=0$ the problem is numerically unstable; results are presented only for $T\geqslant 0.1$. The large dot was obtained for $R=23$ using Eq. (15) and $10^5$ random field configurations. In the shaded region the result of Ref. [3] for the existence of a unique paramagnetic phase applies. The gray dashed lines are the ferromagnetic and the antiferromagnetic lines [4] (cf. also Ref. [3]) and the gray dash-dotted line is Bruinsma's lower bound for the existence of a stable ferromagnetic phase [4]. ($J=1$.)

$$\mathbb{E}_{\{\sigma\}}(g^+-g^-)\leqslant\sum_{\{\sigma\}_R}\sum_{y\in\partial V_R}\prod_{l=0}^{R-1}A'^{(R)}_{z_l(y)_{\max}}\int_{\{\tilde{\sigma}\}_R=\{\sigma\}_R}d\eta(\{\tilde{\sigma}\})\times(g_y^+-g_y^-). \tag{12}$$

The remaining integral for each $y$ is bounded from above by $2^{-|V_R|}\mathbb{E}_R$ where $\mathbb{E}_R=\max_{y\in\partial V_R}\mathbb{E}_{\{\sigma\}}(g_y^+-g_y^-)$ (see Appendix subsection 2). We therefore obtain

$$\mathbb{E}_0=\mathbb{E}_{\{\sigma\}}(g^+-g^-)\leqslant\sum_{\{\sigma\}_R}2^{-|V_R|}\sum_{y\in\partial V_R}\prod_{l=0}^{R-i}A'^{(R)}_{z_l(y)_{\max}}\mathbb{E}_R. \tag{13}$$

The finite sums commute and as $A'^{(R)}_{z_l(y)_{\max}}$ is obtained with homogeneous boundary conditions the sums $\Sigma_{\{\sigma\}_R}$ are identical for all $y\in\partial V_R$, such that the sum over $y$ can be replaced by a factor $|\partial V_R|=k^R$, yielding

$$\mathbb{E}_0\leqslant K\mathbb{E}_R, \tag{14}$$

where

$$K:=\sum_{\{\sigma\}_R}2^{-|V_R|}k^R\prod_{l=0}^{R-1}A'^{(R)}_{z_l(y)_{\max}}. \tag{15}$$

Because of the translation invariance of the Bethe lattice these considerations can be applied recursively. This implies $\mathbb{E}_0\leqslant K^r\mathbb{E}_{r\cdot R}$. If the factor $K$ is less than 1 for any parameters $(T,h)$ we immediately obtain $\mathbb{E}_0=\mathbb{E}_{\{\sigma\}}(|g^+-g^-|)=0$ as $\mathbb{E}_{r\cdot R}$ is uniformly bounded by $2g_+^*$ for all $r\in\mathbb{N}$ and therefore $K^r\mathbb{E}_{r\cdot R}\to 0$ for $r\to\infty$. By translation symmetry this result holds for all $g_y$ with $y\in V$. As $|g^+-g^-|\geqslant 0$ the vanishing expectation even implies $|g^+-g^-|=0$ for almost all realizations $\{\sigma\}$ of the random field.

The reason for using $g_y$ instead of $x_y$ is now easily explained. If we used the effective fields $x_y$ instead of $g_y$ the product over derivatives of $A$ would be from $l=1$ up to $R$. This gives a less precise estimate because $x_y$ with $y\in\partial V_R$ is less restricted than $x_{y_0}$ and therefore the bound for $A'(x_y)$ with $y\in\partial V_R$ is greater than the one for $A'(x_{y_0})$.

To apply the criterion obtained above we evaluated $K$ on a computer. The calculation time is proportional to the number of random field configurations on $V_R$ and thus grows asymptotically for, e.g., $k=2$, as $2^{2^R}$. Therefore, the calculation was restricted to $R\leqslant 4$ (for $R=5$ each data point in an array of $20\times 40$ points would take about 3 days on a Pentium II 350 MHz). The solid line in Fig. 2 shows the upper bound for the existence of a unique paramagnetic phase obtained for $R=4$.

To estimate the results for $R>4$ we relied on statistical methods and sampled random field configurations. When doing so, it is saving time not to exploit the symmetry and to use Eq. (13) instead of Eq. (15). The resulting bound for $R=11$ and a sample of $10^4$ random field configurations is the dashed line in Fig. 2.

As the bound obtained depends systematically on the radius $R$ it is tempting to try to extrapolate to $R=\infty$. For $T=1.2$ we obtained an extremely good fit for the data sampled

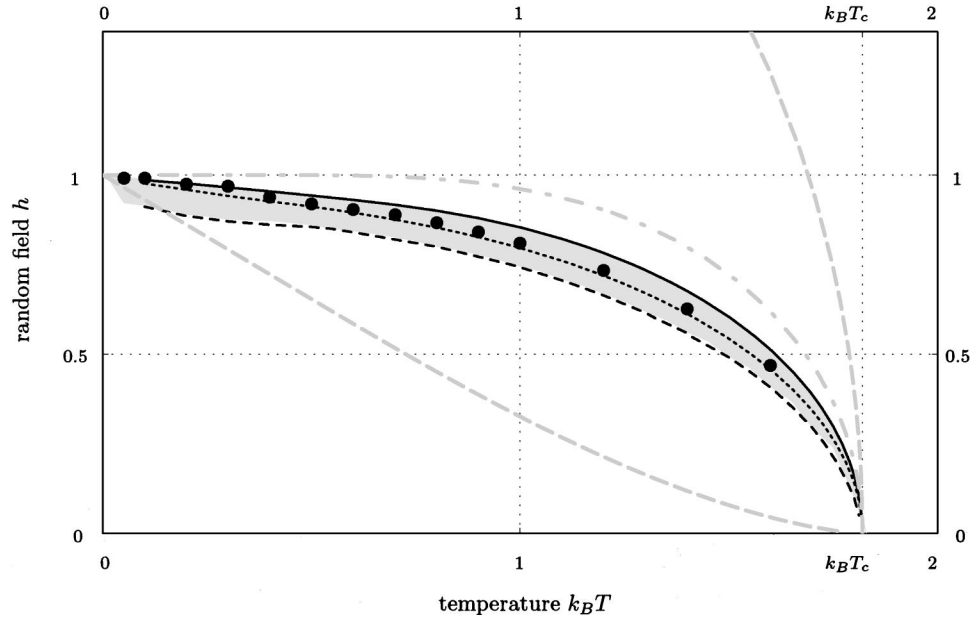


FIG. 3. Estimates for the transition line between para- and ferromagnetism. The dashed line separates regions where the average magnetization decreases or increases with the distance from the boundary for homogeneous boundary conditions $x^b \equiv 0.01$ obtained by comparing the configurational averages over $4\times10^5$ up to $64\times10^5$ samples at distances 9 and 13 from the boundary. The dotted line gives the boundary of the region in which iteration (4) is contractive on the average above and noncontractive below. It was obtained by sampling $10^5$ field configurations and evaluating Eq. (18) with $R=13$ and $R_1=4$. The solid line was obtained using Eq. (23) at $R=4$. The big dots were obtained by evaluating Eq. (24) for $R=20$ and between $10^5$ and $2.4\times10^6$ random field configurations. The gray lines are as in Fig. 2. The gray shaded region marks the region in which all our numerical results (including considerably more than shown explicitly here) are contained. ($k=2$, $J=1$.)

at $R=5,\ldots,23$ using $h_c(R)=a+bR^c$. However, the result was $a=h_c(\infty)\approx 0$, which is not realistic. Other fits, e.g., omitting data for small $R$ or using different functional forms, yielded values between $-0.9$ and 0.45. We suspect that a naive choice of the functional form of $h_c(R)$ does not allow realistic extrapolation results for these bounds in the case of the Bethe lattice.

## IV. ESTIMATES FOR THE TRANSITION LINE

### A. Direct calculation of the magnetization

Even though the bounds presented in the preceding section considerably improve former analytical results, they are still far away from the region where the phase transition from paramagnetic to ferromagnetic behavior is suspected. In Ref. [4] Bruinsma claimed to have found a lower bound in $h$ for the existence of a ferromagnetic phase which is in the relevant parameter region, cf. Fig. 2. To check this bound and to get a good numerical approximation of the transition line we developed several numerical criteria for the existence of a ferromagnetic phase or the existence of a stable paramagnetic phase.

The most obvious criterion for the existence of a ferromagnetic phase is a nonvanishing expectation value for the magnetization for small but nonzero boundary conditions. The expectation value for the local magnetization at the spin in the center is given by

$$m := \mathbb{E}_{\{\sigma\}}\langle s_{y_0}\rangle = \int d\nu(x)\,d\nu(y)\tanh[\beta(x+g(y))] \quad (16)$$

where $\langle\cdot\rangle$ denotes the thermodynamic average, $\mathbb{E}_{\{\sigma\}}$ is the expectation value with respect to all random field configurations, and $\nu$ is the limit measure of the effective field for homogeneous boundary conditions $x_y^b \equiv x^b$ for all $y\in V$ in the limit $R\to\infty$. To approximate $\nu$ we generated a large number of random field configurations on a finite region $V_R$ and calculated the corresponding effective field $x_{y_0}^{(R)}$. The values obtained were then sorted into small boxes of length $\varepsilon$. The resulting histogram was used as an approximation of $\nu_{y_0}(b_i) =: \nu_i$, where $b_i$ is the $i$th box. Explicitly, this yields for the magnetization

$$m \approx \sum_i \sum_j \nu_i \nu_j \tanh\beta(x_i+g(y_j)), \quad (17)$$

where the points $x_i$ and $y_j$ were chosen as the centers of boxes $i$ and $j$, respectively.

Assuming that the magnetization in the center varies monotonically with the radius $R$ of the finite volume $V_R$, one would expect to observe a monotonically increasing magnetization in the ferromagnetic regime and a monotonically decreasing magnetization in the paramagnetic regime for increasing $R$. Therefore, the dashed contour in Fig. 3, which divides the regions in which the numerical estimates of the magnetization are increasing or decreasing with increasing $R$, is a good estimate for the transition line. This type of estimates depends only slightly on the chosen boundary condition and iteration depth but the results obtained significantly disagree with Bruinsma's bound.

### B. Average contractivity of the RIFS

For zero boundary conditions there is a paramagnetic state for any temperature $T$ and random field strength $h$. The stability of this state is tied to the average contractivity of RIFS (4). If it is globally contracting the paramagnetic state is stable and unique. If it is at least contracting on the average for some interval around zero, the paramagnetic phase is stable but the existence of other stable phases is not excluded *a priori*. The investigation of the contractivity of the RIFS was first proposed in Ref. [17].

We generated a set $\Sigma_R$ of random field configurations $\{\sigma\}_R$ on a finite ball $V_R$ and calculated the image of a small initial interval $I^b=[-x^b,x^b]$. Because of the monotonicity of $f_{\{\sigma\}_R}$ the image of this interval at vertex $y$ is $I_y=[x_y^{(R)}(-x^b),x_y^{(R)}(x^b)]$. To estimate the average contractivity of the RIFS we compared the average length $1/k^{R_1}\Sigma_{y\in\partial V_{R_1}}|I_y|$ at the vertices $y\in\partial V_{R_1}$ to the length $|I_{y_0}|$ at the central vertex $y_0$. As the effective fields at all $y\in\partial V_{R_1}$ contribute to the effective field at $y_0$, we consider the average interval lengths at vertices in $\partial V_{R_1}$ instead of individual values. To minimize the influence of the somewhat arbitrary choice of the initial interval the comparison was performed for $R_1\ll R$.

There are two ways of performing the comparison. Either one first averages over the lengths $|I_y|$ at all $y\in\partial V_{R_1}$, then calculates the quotient of $|I_{y_0}|$ and this average length in $\partial V_{R_1}$, and averages over the sample $\Sigma_R$ of random field configurations at the end,

$$\left\langle \frac{|I_{y_0}|}{1/k^{R_1}\Sigma_{y\in\partial V_{R_1}}|I_y|}\right\rangle_{\Sigma_R}, \tag{18}$$

or one first averages $|I_y|$ over all $y\in\partial V_{R_1}$ and all random field configurations as well as $|I_{y0}|$ over the same random field configurations, and calculates the quotient at the end,

$$\frac{\langle|I_{y_0}|\rangle_{\Sigma_R}}{1/k^{R_1}\Sigma_{y\in\partial V_{R_1}}|I_y|\rangle\Sigma_R}. \tag{19}$$

The two averaging procedures (18) and (19) yield identical results and thus obviously are equivalent.

If the images of the initial interval contract on the average for a finite iteration of Eq. (4) we expect complete contraction to length zero for infinite iteration. This corresponds to a stable paramagnetic phase. Therefore, the contour in the $(T,h)$ parameter plane at which the average quotient of band lengths switches from greater than 1 below to less than 1 above is an estimate for the stability region of the paramagnetic phase. The resulting estimated transition line is shown for $R=13$, $R_1=4$, the initial interval $I^b=[-0.01,0.01]$, and $10^5$ random field configurations as the dotted line in Fig. 3. Again, the agreement of the obtained results for various boundary conditions and iteration depths is satisfactory but there is a large deviation from Bruinsma's line.

### C. Independence of the effective fields from boundary conditions

A related criterion for the existence of a stable paramagnetic phase is the independence of the effective field from boundary conditions. As in Sec. III we use the effective fields $g_y^{(R)}$ rather than $x_y^{(R)}$. We consider boundary conditions $\{g_y^b\}_{y\in\partial V_R}$, taking values in a small interval $[-g^b,g^b]$. Through the iteration with Eq. (4) the effective fields $g_y^{(R)}$ are functions of the boundary conditions

$$g_y^{(R)}=\tilde{f}_{\{\sigma\}_{R-n-1}(y)}(\{g_z^b\}) \tag{20}$$

where the function $\tilde{f}_{\{\sigma\}_{R-n-1}(y)}$ has $k^{R-n}$ arguments for $y\in\partial V_n$ and is the identity if $R=n$. For simplicity and without loss of generality we restrict the following discussion to $g_{y0}^{(R)}$. The boundary conditions can be written as $g_y^b=g^b\hat{g}_y^b$ where $\hat{g}_y^b$ takes values in $[-1,1]$. To investigate how the effective fields depend on the boundary conditions we consider the expectation value of the derivative of $g_{y0}^{(R)}$ with respect to $g^b$, the *strength* of the applied boundary condition,

$$\begin{aligned}\mathbb{E}_{\{\sigma\}_{R-1}}\left|\frac{d}{dg^b}g_{y_0}^{(R)}\right| &\leq \mathbb{E}_{\{\sigma\}_{R-1}}\sum_{y\in\partial V_R}\partial_{g_y}\tilde{f}_{\{\sigma\}_{R-1}}(\{g_z^b\}_{z\in\partial V_R})|\hat{g}_y^b| \\ &\leq \sum_{y\in\partial V_R}\mathbb{E}_{\{\sigma\}_{R-1}}\prod_{l=0}^{R-1}A'(x_{z_l(y)}^{(R)}(x^b))\end{aligned} \tag{21}$$

where $x_{z_l(y)}^{(R)}(x^b)$ denotes the effective field along the unique path from $y$ to $y_0$ with homogeneous boundary conditions $x_y^b\equiv A^{-1}(g^b)$. Now one can estimate, as in Appendix A 1,

$$\begin{aligned}A'[x_{z_l(y)}^{(R)}(x^b)] &\leq \min\{A'(\max\{x_{z_l(y)}^{(R)}(x^b),0\}), \\ &\quad A'(\min\{x_{z_l(y)}^{(R)}(-x^b),0\})\} \\ &=: A'^{(R)}_{z_l(y)_{\max}}(x^b).\end{aligned} \tag{22}$$

As the boundary conditions are homogeneous this implies that

$$\mathbb{E}_{\{\sigma\}_{R-1}}\left|\frac{d}{dg^b}g_{y_0}^{(R)}\right| \leq k^R\mathbb{E}_{\{\sigma\}_{R-1}}\prod_{l=0}^{R-1}A'^{(R)}_{z_l(y)_{\max}}(x^b). \tag{23}$$

If the right-hand side vanishes for $R\to\infty$ the effective field $g_{y_0}$ is on the average independent of boundary conditions, taking values in $[-g^b,g^b]$. By determining the parameter region in which the right-hand side of Eq. (23) vanishes for $R\to\infty$, we therefore get an upper bound on the emergence of a stable paramagnetic phase. As our calculations are limited to finite $R$, convergence to zero is assumed if the obtained values of Eq. (23) for $R>0$ are smaller than 1, which is the value for $R=0$.

For the Bethe lattice of degree $k=2$, radius $R=4$, and $g^b=0.01$, the right-hand side of Eq. (23) was evaluated. The contour between values smaller than 1 above and greater than 1 below is shown as the solid line in Fig. 3. For $R>4$

we again relied on sampling random field configurations instead. The resulting transition lines for various iteration depths and boundary conditions are comparable to the results of the preceding two sections and are all contained in the gray region in Fig. 3.

If we consider the derivative of the effective field at $y_0$ in the case of boundary conditions $g^b \equiv 0$ we have

$$\mathbb{E}_{\{\sigma\}_{R-1}} \frac{dg_{y_0}^{(R)}}{dg^b}(\{0\}) = \mathbb{E}_{\{\sigma\}_{R-1}} \sum_{y \in \partial V_R} \prod_{l=0}^{R-1} A'(x_{z_l(y)}^{(R)}(\{0\})). \tag{24}$$

If this derivative does not tend to zero for some parameters $(T,h)$ and $R \to \infty$ there is no stable paramagnetic phase. By determination of the parameter region in which this is the case we get a lower bound on the emergence of a stable paramagnetic phase. The numerical results are the large dots in Fig. 3.

## V. DISCUSSION

In order to interpret the discrepancies between Bruinsma's result and our numerical investigations we briefly review Bruinsma's argument [4] in our language.

The probability measures $\nu_y$ of the effective fields $x_y$ are fixed points of the Frobenius-Perron equation, Eq. (7). They can be approximated by finite iterations of some initial probability densities (boundary conditions) $\nu_y^b$ for $y \in \partial V_R$. If the support of $\nu_y^b$ is a subset of the invariant interval $I$, the support of $\nu_{y_0}$ is a subset of the images of $I$ by functions $f_{\{\sigma\}_R}$. These images are called *bands*. The left and right boundaries of the bands are the effective fields corresponding to homogeneous boundary conditions $x_y^b \equiv x_+^*$ and $x_y^b \equiv x_-^*$ for $y \in \partial V_R$, respectively. The investigation of the structure of the set of bands has proved to be a powerful tool in the treatment of the one-dimensional random field Ising model [8–16]. In contrast to the one-dimensional case, the bands are highly degenerate here, i.e., different configurations of the random field result in the same band. This is due to the invariance of the model with respect to permutations of subtrees for homogeneous boundary conditions. The most degenerate bands correspond to the two *chessboard* configurations (see Fig. 4) of the random field with $+h$ or $-h$ at $y_0$, respectively. There are $2^{2^{R-1}-1}$ equivalent random field configurations in the case of the Bethe lattice of degree $k=2$ and radius $R$. As the total number of configurations is $N=2^{2^R-1}$ the most degenerate bands have a weight of $2^{2^{R-1}-1}/2^{2^R-1} = 2^{-2^{R-1}} \sim 1/\sqrt{N}$. The bands with the least weight are the bands corresponding to homogeneous $+h$ or $-h$ random field configurations. They have the weight $1/N$. The weights of all other bands are distributed between these values.

Bruinsma used boundary conditions $\nu_y^b \equiv \delta_{x^b}$ for some $x^b \in \mathbb{R}$ and iterated Eq. (7). He considered only the lowest and highest weight terms corresponding to the least and the most degenerate bands. The highest weight terms obey a recursion relation. The fixed points of this relation can be calculated and it is straightforward to determine for which temperatures $T$ and random field strengths $h$ they are symmetric about the origin. Proving differentiability of the density $\rho$ of the invariant measure $\nu$ in a neighborhood of $T=T_c$ and $h=0$, Bruinsma concluded that an asymmetric position corresponds to asymmetric maxima of $\rho$ of nonzero weight and therefore to the existence of a ferromagnetic phase.

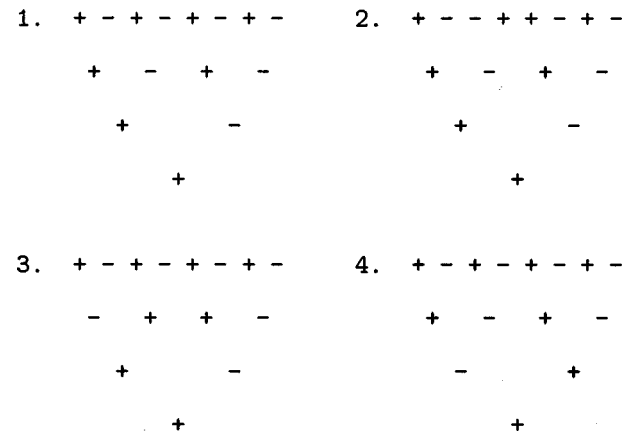


FIG. 4. Four equivalent chessboard configurations at $R=4$. The second configuration is obtained from the first by permutation of two subtrees of a vertex in the sphere $\partial V_2$, the third one by permutation of two subtrees of a vertex in the sphere $\partial V_1$, and the last one by permutation of the two subtrees of the root itself.

The symmetric position corresponds to complete contraction of the most degenerate bands such that the asymmetric boundary condition has no effect in the limit of infinite iteration. The asymmetric position, on the other hand, occurs if the most degenerate bands do not completely contract. Seen this way the argument above is our criterion of average contractivity of the RIFS in Sec. IV B except that it is restricted to the contractivity of one specific band instead of the average contractivity.

There are two problematic points in the reasoning above. First, it is not clear whether the location of local maxima in a differentiable measure density really is given by the most degenerate bands. For small $h$ this actually seems not to be the case; see Fig. 5(a). As the maxima are at $\pm h$ and therefore close to zero for small $h$, it is difficult to argue based on numerical data though. The example in Fig. 5(b) shows, however, that the maxima *are* present for sufficiently large $h$.

Secondly, the differentiability of the invariant measure density has been proved only in a neighborhood of $T=T_c$ and $h=0$ whereas for large $h$ or small $T$ the measure density $\rho$ is clearly *not* differentiable. It is unclear whether it is differentiable in the region of the lower bound; see Fig. 5(b).

The disagreement of our numerical work with Bruinsma's lower bound therefore allows two interpretations. Either Bruinsma's bound is not true outside the proven region of validity because the most degenerate bands are not a sufficient indicator for the symmetry of $\rho$ when the measure density is not differentiable; or in the region between our upper bounds for the existence of a stable paramagnetic phase and Bruinsma's lower bound for the onset of ferromagnetism a stable paramagnetic phase coexists with the (also stable) ferromagnetic phases. This would imply the existence of a first order phase transition and hysteresis loops depending on the strength of the random field, in contrast to the hysteresis at

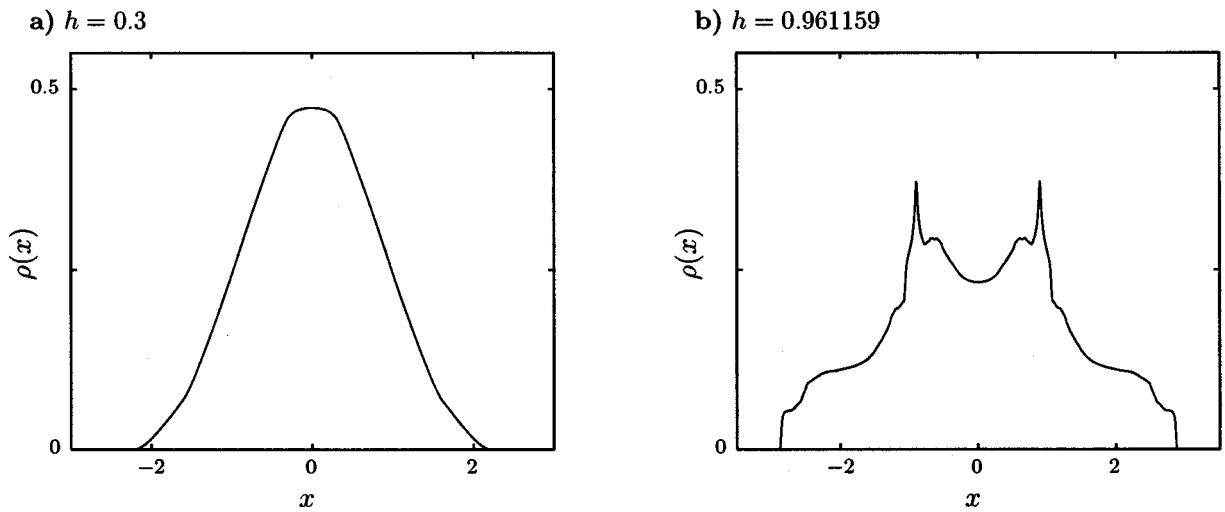


FIG. 5. Approximations of the invariant measure density $\rho$ obtained from fourfold application of Eq. (7) to the equipartition $\rho^b = |I|^{-1}\mathbf{1}_I$ on the invariant interval $I$. There are no maxima at $\pm h$ in (a) whereas the two maxima at $\pm h$ in (b) are already so pronounced that differentiability of $\rho$ is questionable. The random field strength in (b) was chosen such that the point $(T,h)$ is very close to Bruinsma's bound. $(k=2,\ \beta=J=1.)$

$T=0$ [21], which depends on the homogeneous offset of the random field.

In this paper we improved exact upper bounds for the existence of a unique paramagnetic phase in Sec. III, which is a further step toward the exact determination of the phase diagram of the RFIM on the Bethe lattice. Furthermore, we presented numerical work leading to various estimates for the actual phase transition line. The direct calculation of the expectation value of the local magnetization in Sec. IV A, the investigation of the average contractivity of RIFS (4) at large iteration depths in Sec. IV B, and the numerical calculation of the derivative of the effective field with respect to the strength of the boundary condition in Sec. IV C provided estimates for the stability region of the paramagnetic phase. All results are in good agreement while all disagree with the earlier result of Bruinsma [4]. This disagreement motivates further investigations into whether the bound for the onset of ferromagnetism given in Ref. [4] needs to be reconsidered or whether there really is a coexistence region for stable ferromagnetic and a stable paramagnetic phase.

## ACKNOWLEDGMENTS

The work was partially supported by the Cusanuswerk and the DFG (Graduiertenkolleg "Quantenfeldtheorie").

## APPENDIX

### 1. Bound on the partial derivatives in Eq. (11)

The partial derivatives in Eq. (11) are given by

$$\partial_{g_y}\tilde{f}_{\{\tilde{\sigma}\}_{R-1}}(\{\delta_z\}_{z\in\partial V_R}\}) = \prod_{l=0}^{R-1} A'(f_{\{\tilde{\sigma}\}_{R-1-l}[z_l(y)]} \times(\{\varepsilon_z\}_{z\in\partial V_R})), \tag{A1}$$

where $\varepsilon_z = A^{-1}(\delta_z)$, $z_l(y)\in\partial V_l$ are the vertices along the unique path from $y$ to $y_0$ (cf. also Fig. 1), and $\{\tilde{\sigma}\}_{R-1-l}[z_l(y)]$ are the signs of the random field configuration on the subtree of depth $R-1-l$ with root $z_l(y)$. The terms $f_{\{\tilde{\sigma}\}_{R-1-l}[z_{l(y)}]}(\{\varepsilon_z\}_{z\in\partial V_R})$ are effective fields $x^{(R)}_{z_l(y)}$ corresponding to boundary conditions $\{x^b_z=\varepsilon_z\}_{z\in\partial V_R}$. We write $x^{(R)}_{z_l(y)}(\varepsilon)$ for these fields and $x^{(R)}_{z_l(y)}(x^+)$ and $x^{(R)}_{z_l(y)}(x^-)$ for the corresponding effective fields with boundary conditions $x^b_z = x^+_z$ and $x^b_z = x^-_z$ for $z\in\partial V_R$. We can then estimate

$$\begin{aligned} &A'(x^{(R)}_{z_l(y)}(\varepsilon)) \\ &\quad\leqslant \max\{A'(x^{(R)}_{z_l(y)}(\varepsilon'))\,|\,\varepsilon'_z\in[x^-_z,x^+_z], z\in\partial V_R\} \\ &\quad= \max\{A'(x)\,|\,x\in[x^{(R)}_{z_l(y)}(x^-),x^{(R)}_{z_l(y)}(x^+)]\} \\ &\quad= \min\{A'(\max\{x^{(R)}_{z_l(y)}(x^-),0\}),A'(\min\{x^{(R)}_{z_l(y)}(x^+),0\})\}. \end{aligned} \tag{A2}$$

In the last step we used that the maximum of $A'$ in an interval $[a,b]$ is at $a$ if $a\geqslant 0$, at $b$ if $b\leqslant 0$, and at zero in all other cases. As the effective fields can never be larger than $x^*_+$ and never smaller than $x^*_-$ we can for $z\in\partial V_R$ estimate $x^-_z \geqslant h_z + kA(x^*_-) = x^{(R+1)}_z(x^*_-)$ and $x^+_z \leqslant h_z + kA(x^*_+) = x^{(R+1)}_z(x^*_+)$. This allows us to replace $x^+$ and $x^-$ in the argument of $x^{(R)}_{z_l(y)}$ in Eq. (A2) and with $x^{(R)}_{z_l(y)}[x^{(R+1)}_y(x^*_\pm)] = x^{(R+1)}_{z_l(y)}(x^*_\pm)$ we get

$$\begin{aligned} A'(x^{(R)}_{z_l(y)}(\varepsilon)) \leqslant \min\{&A'(\max\{x^{(R+1)}_{z_l(y)}(x^*_-),0\}), \\ &A'(\min\{x^{(R+1)}_{z_l(y)}(x^*_+),0\})\} \\ =: A'^{(R)}_{z_l(y)_{\max}}. \end{aligned} \tag{A3}$$

Inserting Eq. (A3) into Eq. (A1) then yields

$$\partial_{g_y}\tilde{f}_{\{\tilde{\sigma}\}_{R-1}}(\{\delta_z\}_{z\in\partial V_R})\leqslant\prod_{l=0}^{R-1}A'^{(R)}_{z_l(y)_{\max}}. \tag{A4}$$

### 2. Bounds on the integrals in Eq. (12)

Using the independence of the RVs $g_y$ of the signs $\{\sigma_z\}_{z\in V_R\setminus(y)}$ and denoting the number of vertices in $V_R$ by $|V_R|$, i.e., $|V_R|=(k^{R+1}-1)/(k-1)$, one obtains

$$\begin{aligned}\int_{\{\tilde{\sigma}\}_R=\{\sigma\}_R}d\eta(\{\tilde{\sigma}\})(g_y^+-g_y^-)&\\ =2^{-|V_R|+1}\int_{\tilde{\sigma}_y=\sigma_y}d\eta(\{\tilde{\sigma}\})(g_y^+-g_y^-)&\\ =2^{-|V_R|}\mathbb{E}_{\{\sigma\}}(g_y^+-g_y^-|\tilde{\sigma}_y=\sigma_y).&\end{aligned} \tag{A5}$$

The function $A$ is antisymmetric, which implies $g_y^+(\{-\sigma\})=-g_y^-(\{\sigma\})$ and therefore

$$\mathbb{E}(g_y^+-g_y^-|\sigma_y=+)=\mathbb{E}(g_y^+-g_y^-|\sigma_y=-), \tag{A6}$$

implying

$$\begin{aligned}\mathbb{E}(g_y^+-g_y^-)&=\tfrac{1}{2}\mathbb{E}(g_y^+-g_y^-|\sigma_y=+)+\tfrac{1}{2}\mathbb{E}(g_y^+-g_y^-|\sigma_y=-)\\ &=\mathbb{E}(g_y^+-g_y^-|\sigma_y=\sigma)\end{aligned} \tag{A7}$$

for any $\sigma\in\{-,+\}$. Setting

$$\begin{aligned}\mathbb{E}_R&:=\max_{y\in\partial V_R}\mathbb{E}_{\{\sigma\}}(g_y^+-g_y^-|\tilde{\sigma}_y=\sigma_y)\\ &=\max_{y\in\partial V_R}\mathbb{E}_{\{\sigma\}}(g_y^+-g_y^-),\end{aligned} \tag{A8}$$

this finally yields

$$\int_{\{\tilde{\sigma}\}_R=\{\sigma\}_R}d\eta(\{\tilde{\sigma}\})(g_y^+-g_y^-)\leqslant 2^{-|V_R|}\mathbb{E}_R. \tag{A9}$$


[1] T. Nattermann, in *Spin Glasses and Random Fields*, edited by A. P. Young (World Scientific, Singapore, 1998), p. 277, and references therein.
[2] D. P. Belanger, in *Spin Glasses and Random Fields* (Ref. [1]), p. 251, and references therein.
[3] P. M. Bleher, J. Ruiz, and V. A. Zagrebnov, J. Stat. Phys. **93**, 33 (1998).
[4] R. Bruinsma, Phys. Rev. B **30**, 289 (1984).
[5] R. Bruinsma and G. Aeppli, Phys. Rev. Lett. **50**, 1494 (1983).
[6] G. Aeppli and R. Bruinsma, Phys. Lett. **97A**, 117 (1983).
[7] P. Ruján, Physica A **91**, 549 (1978).
[8] G. Györgyi and P. Ruján, J. Phys. C **17**, 4207 (1984).
[9] U. Brandt and W. Gross, Z. Phys. B **31**, 237 (1978).
[10] P. Szépfalusy and U. Behn, Z. Phys. B: Condens. Matter **65**, 337 (1987).
[11] U. Behn and V. A. Zagrebnov, JINR Report E 17-87-138 Dubna, 1987; J. Stat. Phys. **47**, 939 (1987); J. Phys. A **21**, 2151 (1988); Phys. Rev. B **38**, 7115 (1988).
[12] J. Bene and P. Szépfalusy, Phys. Rev. A **37**, 1703 (1988).
[13] J. Bene, Phys. Rev. A **39**, 2090 (1989).
[14] T. Tanaka, H. Fujisaka, and M. Inoue, Phys. Rev. A **39**, 3170 (1989); Prog. Theor. Phys. **84**, 584 (1990).
[15] U. Behn, V. B. Priezzhev, and V. A. Zagrebnov, Physica A **167**, 481 (1990).
[16] U. Behn and A. Lange, in *From Phase Transitions to Chaos*, edited by G. Györgyi, I. Kondor, L. Sasvári, and T. Tél (World Scientific, Singapore, 1992), p. 217.
[17] H. Patzlaff, Ph.D. dissertation, Universität Leipzig, 1997.
[18] M. R. Swift, A. Maritan, M. Cieplak, and J. R. Banavar, J. Phys. A **27**, 1525 (1994).
[19] U. Brandt, J. Magn. Magn. Mater. **15**, 223 (1980).
[20] H. O. Georgii, *Gibbs Measures and Phase Transitions* (Walter de Gruyter, New York, 1988).
[21] D. Dhar, P. Shukla, and J. P. Sethna, J. Phys. A **30**, 5259 (1997); S. Sabhapandit, P. Shukla, and D. Dhar, J. Stat. Phys. **98**, 103 (2000); P. Shukla, Phys. Rev. E **62**, 4725 (2000); **63**, 027102 (2001).